



ELSEVIER

Human Movement Science 19 (2000) 627–664

HUMAN
MOVEMENT
SCIENCE

www.elsevier.com/locate/humov

Interaction of rhythmic and discrete pattern generators in single-joint movements

Dagmar Sternad^{a,*}, William J. Dean^a, Stefan Schaal^{b,c}

^a *Department of Kinesiology, The Pennsylvania State University, 266 Recreation Building, University Park, PA 16802, USA*

^b *Computer Science and Neuroscience, University of Southern California, Los Angeles, CA 90089-2520, USA*

^c *Kawato Dynamic Brain Project (ERATO/IJST), 2-2 Hikaridai, Saika-Cho, 619-02 Kyoto, Japan*

Abstract

The study investigates a single-joint movement task that combines a translatory and cyclic component with the objective to investigate the interaction of discrete and rhythmic movement elements. Participants performed an elbow movement in the horizontal plane, oscillating at a prescribed frequency around one target and shifting to a second target upon a trigger signal, without stopping the oscillation. Analyses focused on extracting the mutual influences of the rhythmic and the discrete component of the task. Major findings are: (1) The onset of the discrete movement was confined to a limited phase window in the rhythmic cycle. (2) Its duration was influenced by the period of oscillation. (3) The rhythmic oscillation was “perturbed” by the discrete movement as indicated by phase resetting. On the basis of these results we propose a model for the coordination of discrete and rhythmic actions (K. Matsuoka, Sustained oscillations generated by mutually inhibiting neurons with adaptations, *Biological Cybernetics* 52 (1985) 367–376; Mechanisms of frequency and pattern control in the neural rhythm generators, *Biological Cybernetics* 56 (1987) 345–353). For rhythmic movements an oscillatory pattern generator is developed following models of half-center oscillations (D. Bullock, S. Grossberg, The VITE model: a neural command circuit for generating arm and articulated trajectories, in: J.A.S. Kelso, A.J. Mandel, M. F. Shlesinger (Eds.), *Dynamic*

* Corresponding author. Tel.: +814-863-7369; fax: +814-863-7360.
E-mail address: dxs48@psu.edu (D. Sternad).

Patterns in Complex Systems, World Scientific, Singapore, 1988, pp. 305–326). For discrete movements a point attractor dynamics is developed close to the VITE model. For each joint degree of freedom both pattern generators co-exist but exert mutual inhibition onto each other. The suggested modeling framework provides a unified account for both discrete and rhythmic movements on the basis of neuronal circuitry. Simulation results demonstrated that the effects observed in human performance can be replicated using the two pattern generators with a mutually inhibiting coupling. © 2001 Elsevier Science B.V. All rights reserved.

PsycINFO classification: 2330

Keywords: Dynamical systems; Modeling; Rhythmic movement; Discrete movements; Oscillator modeling

1. Introduction

The literature on the control and coordination of limb movements appears to be divided into studies that address target-directed discrete movements, such as reaching for a cup, and studies that investigate continuous rhythmic actions, such as walking and running. While the former class of movements has been addressed in numerous ways from a control theoretical or information-processing perspective (e.g., Flash & Hogan, 1985; Hoff & Arbib, 1993; Jeannerod, 1984; Uno, Kawato & Suzuki, 1989), rhythmic movements have been the central phenomenon investigated by the dynamical systems perspective (Kelso, 1995; Turvey, 1990). The latter focus has been motivated by the tenet that spontaneous rhythmic activity is a primary expression of the nervous system in animals and humans (Brown, 1914; Goodwin, 1970; Iberall, 1972; Yates, Marsh & Iberall, 1972). This position contrasts with the strategy that aims to account for the variety of human and animal behavior by identifying segments in movement trajectories and address the problem of their concatenation (e.g., Lacquaniti, Terzuolo & Viviani, 1983). This empirical and theoretical separation does not pay tribute to the fact that almost every action consists of a combination of translatory and cyclic elements which may occur either in sequence or simultaneously. Playing the piano, itself one of the most intriguing and frequently studied examples of a rhythmic skill, requires not only the precise timing of repeated key strokes but also the translatory action that carries the fingers or hands across the keys. Cursive handwriting is another example that consists of traces rhythmically moving up and down, but it also requires the translatory movement of the pen across the page. Interestingly, this skill has found theoretical

accounts both in terms of a sequential ordering of strokes (Viviani & Terzuolo, 1982), and in terms of coupled oscillations (Hollerbach, 1981; Kalveram, 1998).

There are very few studies that provide an exception to this “dualistic” empirical approach. One line of research where the co-existence of rhythmic and discrete actions has been discussed is the area of tremor. As early as 1929, Travis found that rapid voluntary extension of the forefinger in healthy adults tended to be initiated during the extension phase of the 8–12 Hz physiological tremor. Additionally, the tremor rhythm was found to be disturbed, as if the volitional movement temporarily suppressed it. Similarly, Hallet, Shahani and Young (1977) studied Parkinson patients with a 5 Hz tremor and observed a delay in the initiation of a voluntary action. The authors suggested this delay to be due to a “waiting” for the right time in the tremor cycle. Following these observations, Goodman and Kelso (1983) studied healthy individuals who performed a voluntary isometric finger abduction against the background of physiological tremor (8–12 Hz). The voluntary contraction onset was limited to a phase window of the tremor cycle, specifically, the cycle segment close to peak angular velocity. This effect was observed under metronome-paced and self-paced conditions, both with and without added load attached to the finger. The result was interpreted that for the initiation of the discrete movement biological systems utilize the momentum of the muscle–joint system, and thereby exploit existing cyclicities rather than are perturbed by it (Soodak & Iberall, 1972). In search for an underlying reason for the observed delaying and hastening of rapid tapping movements in Parkinson patients Wierzbicka, Staude, Wolf and Dengler (1993) examined whether the initiation of a single intentional action is attracted to a specific phase in the EMG of the ongoing tremor oscillation. Indeed, the phasic EMG burst is most commonly generated during the second half of the EMG tremor cycle, with the burst occurring slightly earlier than expected in the resting tremor burst. The same group of researchers continued this investigation and found that also reaction time is modulated as a function of the underlying tremor (Staude, Wolf, Ott, Oertel & Dengler, 1995). More recently, this observation was also found to hold for voluntary rhythmic movement in a single joint and across two joints (Latash, 2000). An apparent conflict between Goodman and Kelso’s and Wierzbicka et al.’s results was addressed by Elble, Higgins and Hughes (1994). While Goodman and Kelso’s healthy participants initiated their movements at maximum momentum, the Parkinson patients in Wierzbicka et al.’s study initiated the movement onset in the phase where momentum opposed the movement

direction. Elble et al. (1994) repeated the latter finding in patients with essential tremor (4–8 Hz) arguing that movement onset is a function of oscillation frequency and, thereby, the phase relation between the EMG and kinematic trace which changes as a function of movement frequency. Despite some differences in the quantitative details of their results, all mentioned studies demonstrate an interaction between an ongoing oscillation and a discrete volitional action.

The nature of this interaction was addressed in more detail in a study by Adamovich, Levin and Feldman (1994). When two control commands for a discrete and a rhythmic voluntary action have to be issued to the same effector, are they issued in sequence or simultaneously? If the two types of movements have to co-occur, do the control signals interact at a central level or is there a merging only in the kinematic consequences? Participants performed rapid elbow oscillations (5–7 Hz) around a given target while shifting the mean joint angle to a second target in a fast point-to-point movement. Again, the discrete movement's onset was predominantly confined to a narrow phase window of the preceding oscillation. Using averaging techniques on the kinematic and EMG traces, the discrete movement appeared to be unaffected by the rhythmic movement. In reverse, the rhythmic movement was temporarily suppressed as evidenced by a shifting of phase. Adopting the framework of the equilibrium hypothesis, these two findings were interpreted to conclude that two control signals for the discrete and the rhythmic movement were issued in sequence, due to conflicting stability requirements of the *r* and *c* command. Overlapping features were due to merging of mechanical consequences at the periphery. This conclusion remains unsatisfactory in light of the observation that within everyday behavioral activities many rhythmic and discrete actions occur simultaneously. The goal of this paper is to propose that similar results can be the consequence of the parallel interaction of dynamic units, or pattern generators, that produce discrete and rhythmic behaviors.

Adopting a dynamical systems' perspective, accounts for discrete actions have been sparse. A first attempt was advanced by Schöner (1990) who proposed a dynamical model in which a discrete movement is one of several regimes in the parameter space. Whether the system displays limit cycle or point attractor behavior is defined by a set of parameter values. While the study demonstrates in an exemplary fashion how limit cycle modeling can be extended to discrete movements, the motivation for the suggested model equation rested on purely formal grounds to keep the equation analytically tractable. In order to address the serial ordering of movements Sternad,

Saltzman and Turvey (1998) proposed a multi-layered dynamical model. The methodological strategy was to modify the cyclic bimanual actions to gradually extend the modeling framework and capture discrete and serial aspects of a behavioral sequence. The particular task involved one effector, a hand–pendulum system, performing an ongoing cyclic action, while the other hand–pendulum performed one discrete cycle with every fourth cycle of the continuous oscillation. The kinematic interaction effects observed across hands were modeled on three layers: The model level consisted of a damped oscillation for the “discrete” cycle and an autonomous oscillation for the continued rhythmic motion coupled together. These two oscillatory units in turn drove the biomechanical or peripheral level that captured the pendulum dynamics. The task parameters were specified on the task level where a parameter dynamics was determined. While this study modified strictly rhythmic behavior and could produce sequential overlapping effects, the single action was still a cycle and not a truly discrete point-to-point movement. For two related multi-level approaches see Saltzman and Kelso (1987) and Schöner (1995), who addressed the problem of trajectory formation in a more general framework in which the mass-spring model was generalized onto a task level as well as a biomechanical or load level.

The objective of the present study is to propose a dynamical account for discrete and rhythmic movements and specifically their interaction. A framework is suggested that allows to address movements that consist of both a translatory and a cyclic component. The more fundamental reasoning behind this is the proposition that rhythmic and discrete patterns form the two elementary units of action. Every degree of freedom, assumed to be defined in joint space, is able to move either in a discrete or a rhythmic fashion. This hypothesis is motivated by the fact that nonlinear dynamical systems have two fundamental stable regimes, a point attractor and a limit cycle attractor. The presented experiment investigates a movement task similar to the one studied by Adamovich et al. (1994) which combines rhythmic and discrete elements. Kinematic and electromyographic data are analyzed with a view to how the rhythmic and discrete actions influence each other. On the basis of these results a modeling framework for discrete and rhythmic pattern generators is suggested with the hypothesis that these units act as movement primitives or units of action. To address the interaction of rhythmic and discrete actions, point attractor dynamics and limit cycle dynamics are coupled. Simulation results show how a mutually inhibitory coupling between the two units can reproduce the data.

2. Method

2.1. Participants

There were nine participants, graduate and undergraduate students and one faculty member from The Pennsylvania State University that volunteered (7 male, 2 female). Their age ranged from 20 to 45 years. All reported themselves to be right-hand dominant and to have no history of serious injury to their right arms. Prior to data collection, the participants were informed about the experimental procedure and signed the consent form in agreement with the University's Regulatory Committee. Data of one more participant was collected but as she did not maintain the frequency prescribed by the metronome, her data was discarded.

2.2. Experimental apparatus and data collection

The participant was seated in front of a table with his/her right forearm placed horizontally on a foam-padded metal support affixed to an axle. The height of the chair was adjusted so that the upper arm was horizontal and at the same height as the forearm. The center of rotation of the elbow joint was aligned with the axle of the apparatus. As the chest rested against the table, shoulder movements were minimized and elbow flexion and extension occurred in the horizontal plane. The participants grasped a wooden dowel affixed to the end of the arm support with their right hand. To ensure a fixed forearm position a Velcro band strapped the forearm moderately tightly to the support arm. Two vertical targets (wooden rods of 15 cm height) were placed on the table on a circular arc, whose origin was at the elbow joint and whose radius extended approximately 10 cm beyond the fingertips. Target 1 (T1) was positioned where the elbow was flexed by 60° from full extension which was defined to be 180°. Therefore, T1 was at 120°. Target 2 (T2) was placed at 60°, 120° from full extension. The target markers also had horizontal bars, attached in a cross-like fashion, which indicated the oscillation amplitude of 20°, measured from minimum to maximum. A computer-generated metronome signal set the oscillation frequencies for the initial phase of the movement task (beep duration: 100 ms, pitch frequency: 770 Hz). After 6–10 cycles of silence, another metronome beep (200 ms, 1000 Hz) signaled the onset of the discrete movement. The end of the data collection was indicated by a third type of metronome beep (300 ms, 500 Hz).

Data of joint angular position were collected by an optical encoder (US Digital H3-2048) affixed to the axle of the apparatus. The rotational resolution of the optical encoder was 0.044° . The sampling frequency was 420 Hz, controlled by a 555 timing circuit wired to oscillate in an astable mode. Electromyographic data were collected from two elbow flexors and two elbow extensors: the long head of the biceps brachii (BB), the brachio-radialis (BR), the lateral head of the triceps (TLA) and the long head of the triceps (TLO) of the right arm, respectively. The sampling frequency was also 420 Hz and controlled by the same timing circuit. In addition to the EMG and kinematic signals, the output of the speaker was recorded to provide information about the temporal onset of the metronome signals. Concurrently, the output of a switch circuit was recorded, which was closed only when the elbow was fully extended. Flexing the arm opened this circuit and this event was used to time-align the analog EMG data and the data of the optical encoder. The collection of all signals was controlled by LabView Software (National Instruments) on a Macintosh Computer (PowerCenter Pro 210, Power Computing).

2.3. *Experimental conditions*

Before the beginning of each trial the participant fully extended his elbow (to close the switch circuit) and was instructed to begin oscillating around one of the targets as indicated by the experimenter. He then moved the forearm to the prescribed target and oscillated in synchrony with the auditory metronome generated by the computer. After 10 beats, the metronome signal ceased but the participant continued to oscillate at the same prescribed frequency until he heard another computer-generated tone. The participant was instructed that upon hearing this tone he was to “. . . shift [his] oscillation to the other target as fast as possible, without stopping the ongoing rhythmic movements.” This instruction emphasized both the reaction to the signal to be “as fast as possible” as well as the fact that the displacement between targets should be as fast as possible. This instruction was so designed to force the participants to combine both rhythmic and discrete actions. The onset of the beep occurred randomly in a window between 3 and 8 cycle periods after cessation of the pacing metronome. The participant continued to oscillate around the second target until another tone signaled the end of the trial. Each trial lasted 15 seconds.

The experimental conditions were presented in a 2×2 design: (1) The initial oscillation frequency set by the metronome was either 2 or 3 Hz. (2) The movement was performed with either elbow flexion, from T1 to T2,

or extension, from T2 to T1. The oscillation amplitude around each target was identical. Each participant performed 10 trials under each of the four conditions. The order of presentation was fully randomized.

2.4. Data reduction and analysis

The digitized EMG signals were rectified and filtered using a sixth-order low-pass Butterworth filter with a cut-off frequency of 35 Hz. The joint angle data did not have to be filtered, as the optical encoder signals were extremely smooth. For each of the four muscles measured, the timing of each activity burst during the rhythmic movement was calculated. For this purpose, the EMG signals were divided into windows delineated by the joint angle excursions. For the flexion trials, which started with oscillations around T1, and the elbow flexors, BB and BR, acted as agonists, the windows were defined by the minima of the elbow angular excursion (for an exemplary flexion trial see Fig. 1). For the extension trials, where the two extensors TLA and TLO acted as agonists, the window markers were set by the maxima of the angular displacement. Within each window, the time of the onset and the peak of the burst as well as the peak amplitude were determined. The onset was defined where the EMG signal significantly exceeded the baseline. These calculations were performed for both flexors and both extensors. On the whole the results of both muscles were very similar. The calculations were first conducted algorithmically on the basis of the criteria. To confirm its correctness, they were subsequently checked by eye.

2.4.1. Kinematic parameters

For both the intervals preceding and succeeding the discrete movement the individual cycle periods and amplitudes as well as their means were calculated on the basis of the joint angular displacement. To obtain a comparable definition for flexion and extension trials, we used the excursions opposite to the direction of the discrete shift, denoted by A_i (see Fig. 1 for an exemplary flexion trial). The cycles are indexed by numbers, with $-1, -2, \dots$ before, and as $1, 2, \dots$, after the discrete movement. The individual cycle periods of the periodic intervals T_i ($i = \dots, -1, 1, 2, \dots$) were calculated between excursions i and $i - 1$. Subsequently, for each trial the preceding and succeeding periods of three cycles before T_{-3} and three cycles after T_3 were averaged to obtain T_{pre} and T_{post} , respectively. The cycle amplitudes of the rhythmic intervals A_i were calculated as the half-amplitudes calculated from the center of oscillation. This center of oscillation was computed as the average

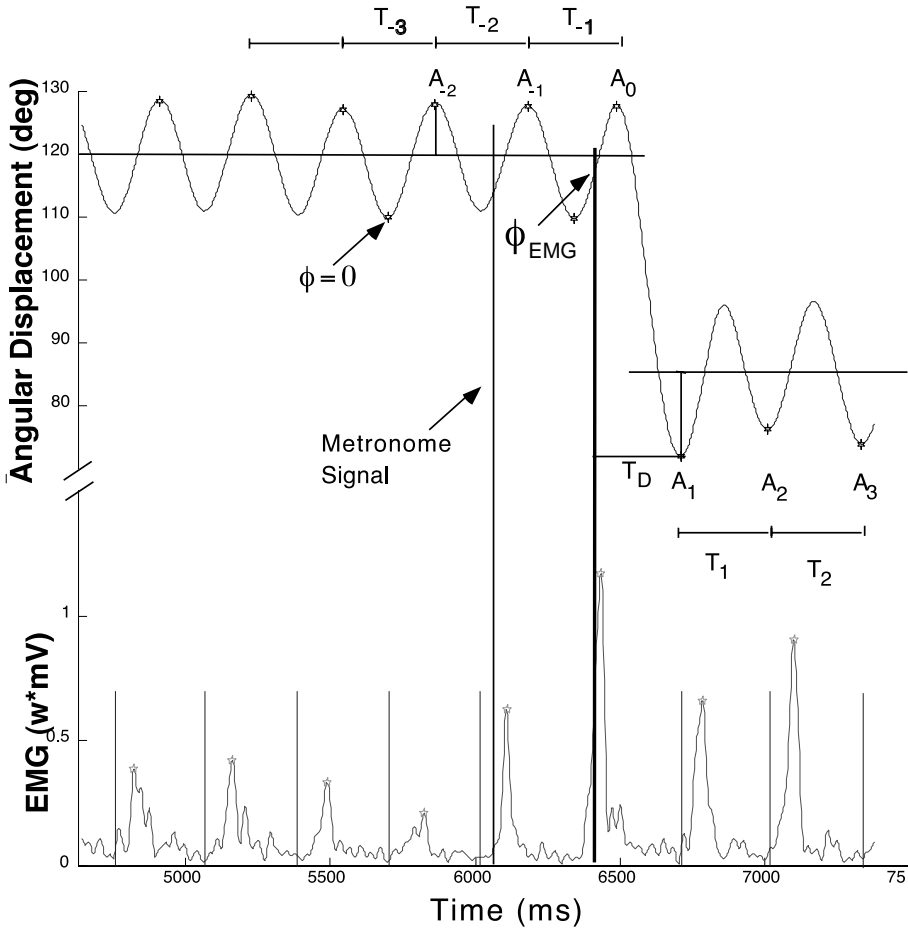


Fig. 1. Segment of a representative time series of joint angle motion and EMG activity of the biceps brachii in a flexion trial performed with oscillations at 2 Hz. The EMG data are in weighted units. For explanation of the notation see text.

displacement of all cycles before A_{-1} and after A_1 separately. Subsequently, A_{pre} and A_{post} were calculated averaging over three cycle amplitudes before A_{-3} , and three cycles after A_3 to obtain amplitude estimates for the first and second oscillatory intervals. To quantify the duration and extent of the discrete movement, a discrete time T_D was calculated between the time of the onset of the discrete movement and A_1 . In addition, mean cycle periods were also calculated on the basis of the EMG signals. τ_{EMG} was calculated as the average time between the peaks of 5 EMG bursts prior to the transition.

2.4.2. Onset of discrete movement

The onset of the discrete movement T_{onset} was determined as the time where the EMG activity exceeded the threshold which was defined as the average peak value of the five bursts prior to the discrete movements plus 1 standard deviation. As first choice for determining these data, the muscles BR and TLA were used. In 36 out of 200 trials BR and TLA did not show peaks of activity preceding the discrete movement that satisfied the above criteria. In these cases, the BB and TLO were checked for qualifying bursts. In all but five cases, qualifying onsets were found in the other agonist. As a check on the accuracy of our calculations the time of onset for the discrete movement was calculated using both flexor and both extensor signals. The difference between the two calculations using each pair of agonists was determined. The differences in onset times averaged out and were close to zero ms. The phase of onset ϕ of the discrete movement relative to the rhythmic oscillation was determined in two ways: (1) on the basis of the joint angle data: ϕ_{ANGLE} . (2) On the basis of the EMG data: ϕ_{EMG} . To obtain ϕ_{angle} a ΔT was calculated as the time between T_{onset} and the valley three cycles prior to the transition (see Fig. 1):

$$\Delta T = t_{\text{valley},3} - t_{\text{onset}}.$$

ϕ_{angle} was then obtained according to:

$$\phi_{\text{angle}} = 2\pi \left(\frac{\Delta T \bmod T_{\text{pre}}}{T_{\text{pre}}} \right).$$

Note that $\phi_{\text{angle}} = 0$ at the valleys for flexion trials and at the peaks for extension trials.

To obtain ϕ_{EMG} , the analogous algorithm was used. ΔT was calculated as the time between T_{onset} and the peak three cycles preceding the onset.

$$\phi_{\text{EMG}} = 2\pi \left(\frac{\Delta T \bmod T_{\text{EMG}}}{T_{\text{EMG}}} \right).$$

2.4.3. Phase shift

The phase shift $\Delta\phi$ was calculated as follows for the flexion trials:

$$\Delta\phi = 2\pi \left(\frac{t_{\text{valley},2} - (t_{\text{valley},-2} + 3T_{\text{pre}})}{T_{\text{pre}}} \right),$$

where $t_{\text{valley},-2}$ refers to the valley two cycles before the discrete transition, and $t_{\text{valley},2}$ to the second valley after the transition. By adding three cycle periods to $t_{\text{valley},-2}$ the oscillation is projected forward as if unperturbed. This value is subtracted from the actual $t_{\text{valley},2}$ and the time difference is then transformed into phase as shown. For the extension trials, the corresponding peaks prior and post to the transition served as the landmarks.

2.4.4. Reaction time

Premotor reaction time was measured as the time between the onset of the auditory stimulus and the time of the super-threshold EMG activity.

3. Results

Fig. 1 displays a section of a representative time series of joint angle data and EMG data of the biceps brachii (BB) for a flexion trial together with the adopted notation for the kinematic variables. The first long vertical line indicates the onset of the metronome signaling to the participant to shift the center of oscillation from T1 to T2. The second vertical line indicates the onset of the discrete movement as calculated from a super-threshold activation of BB. The short vertical lines in the EMG trace demarcate the segmentation of the EMG signal into cycles determined by the valleys in the joint angle trace. Periods and amplitudes of the oscillatory interval before and after the discrete transition were calculated for each trial as detailed in Section 2. An overview over average periods and amplitudes of five representative participants for the 2 and 3 Hz conditions can be obtained in Fig. 2(a)–(d). The same five participants are shown in all four bar charts. Each bar shows the average across 20 trials performed in both flexion or extension direction. The pooling over these two conditions was warranted because very few participants showed differences between the two movement directions (see analyses below). As to be expected from the instructions, the periods in the 2 Hz condition vary around 500 ms and in the 3 Hz condition around 333 ms. Note that the scale starts at 0.20 seconds to amplify the pattern of changes in the periods within each participant. The corresponding amplitudes in the two frequency conditions show smaller values for the 3 Hz compared to the 2 Hz condition. The following analyses will focus on different aspects illustrated in these four graphs.

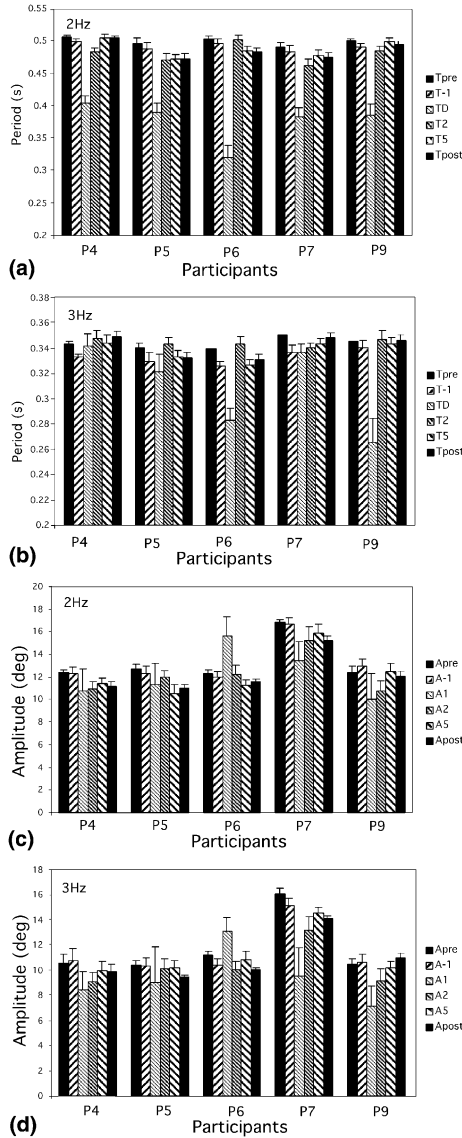


Fig. 2. Period and amplitude means of flexion and extension trials of five selected participants. (a) and (b): The different bars show the mean period in the pre- and post-discrete intervals, T_{pre} and T_{post} , the period directly prior to the discrete movement, T_{-1} , the duration of the discrete movement between onset and the first post-discrete excursion, T_D , the second and fifth period after the discrete movement T_2 and T_5 . (c) and (d): Amplitudes in the pre- and post-discrete intervals, A_{-1} refers to the last amplitude prior to the discrete movement, A_1, A_2 and A_5 denote amplitudes in the respective cycles after the discrete movement. A_{pre} and A_{post} are average amplitudes.

3.1. Perturbation of the ongoing oscillation by the discrete movement

The first set of analyses focuses on the oscillations before and after the discrete movement. Whilst the discrete movement is an explicit component in the movement sequence, it can equally be interpreted as a perturbation of the ongoing oscillation. Is the oscillation maintained or changed in its kinematic characteristics by the discrete movement? To address this question, the average periods and amplitudes preceding and succeeding the transition were compared. The mean pre-discrete periods and amplitudes T_{pre} and A_{pre} were calculated as the average of three cycles prior to A_3 ; the post-discrete averages T_{post} and A_{post} were calculated from the three cycles after A_3 to eliminate transient effects. The period and amplitude means were submitted to a 2 (oscillation frequency) \times 2 (movement direction) \times 2 (pre-/postdiscrete interval) ANOVA, where oscillation frequency and movement direction were entered as between factors, and the pre-post interval was a repeated factor. This analysis was performed for each participant separately, because inter-participant differences were of no interest in this context. The results are summarized in Tables 1 and 2. As the main effect for movement direction was not significant in 7 out of 9 participants, the listed values are means over flexion and extension trials. The main effect for frequency was highly significant in all participants as to be expected ($p < 0.0001$). Across participants some of the two-way interactions were significant, but these effects were unsystematic across participants and will therefore not be further interpreted. Most pertinent for the present question is whether amplitudes and periods are changed after the discrete perturbation. As Tables 1 and 2 highlight, almost all

Table 1

Average periods (ms) per participant in the intervals before (T_{pre}) and after (T_{post}) the discrete movement, and the period spanning the discrete movement, T_{D} ^a

Periods	2 Hz			3 Hz		
	T_{pre}	T_{post}	T_{D}	T_{pre}	T_{post}	T_{D}
P1	508	483	554	336	323	417
P2	500	481	619	346	352	468
P3	509	507	548	341	347	429
P4	492	475	567	334	331	427
P5	502	482	585	333	325	427
P6	484	476	469	344	346	385
P7	512	509	545	342	339	406
P8	494	498	607	339	343	441
P9	515	515	543	313	312	342

^a Each value is the average across 20 trials, collapsing flexion and extension trials together.

Table 2

Average amplitudes (degrees) per participant in the intervals before (A_{pre}) and after (A_{post}) the discrete movement, and the amplitude directly after the discrete movement, A_1 ^a

Amplitude	2 Hz			3 Hz		
	A_{pre}	A_{post}	A_1	A_{pre}	A_{post}	A_1
P1	11.22	11.32	15.75	10.84	10.30	14.56
P2	10.15	10.30	7.39	9.22	9.09	7.13
P3	12.33	11.12	10.76	10.41	9.99	8.45
P4	13.05	11.02	11.31	10.26	10.48	9.04
P5	12.18	11.59	15.65	11.02	10.63	13.13
P6	16.09	15.43	13.48	15.20	14.43	9.54
P7	12.27	11.27	9.41	9.10	7.83	4.02
P8	11.79	11.82	10.00	10.60	10.09	7.11
P9	12.12	11.72	8.23	10.12	9.61	3.35

^a Each value is the average across 20 trials, collapsing flexion and extension trials together.

participants have a tendency to speed up and, concomitantly, to decrease the oscillation amplitude. Although the decrease in period is significant in 5 of the 9 participants, the magnitudes of these drifts were extremely small: the overall average is 10 ms. The amplitudes change systematically with frequency in five participants but again only by the relatively small amount of 0.59° across all participants.

3.2. Transient effects in the oscillatory motion after the discrete movement

The next set of analyses focuses on the cycles immediately following the discrete transition with the goal to estimate to what degree the oscillation is perturbed and how long it takes to return to its steady state oscillations. Was there an overshoot or an undershoot in A_1 ? How quickly was periodicity re-established after the discrete perturbation? Inspection of Fig. 2(c) and (d) reveals that in most cases (8 out of 9 participants) A_1 undershot A_{post} and both the amplitudes and periods were reestablished almost entirely after the first post-discrete cycle. This observation was confirmed by a 2 (oscillation frequency) \times 2 (movement direction) \times 8 (post-discrete amplitude) ANOVA conducted on the amplitude estimates comparing seven individual cycles after the discrete transition with the average A_{post} . The main effect for the repeated variable, the post-discrete amplitudes, was significant in 7 out of 9 participants ($p < 0.0001$). Pairwise Tukey tests identified that this difference existed only between A_1 and A_{post} ; all other cycle amplitudes were not significantly different from A_{post} . Performing the same analysis for the cycle periods revealed identical results: only T_1 was different from the T_{post} (Fig. 2(a) and (b)). This pattern

was systematic in 8 out of 9 participants. Hence, it can be concluded that the perturbing effect of the discrete movement died out after one cycle.

3.3. Effect of the rhythmic onto the discrete movement

3.3.1. Duration of the discrete movement

The next question was directed at the nature of the discrete transition itself: Is there an influence seen from the oscillation onto the discrete movement? The duration of the transition T_D was captured as the time from the onset of the discrete movement to the first excursion A_1 after the discrete movement. Fig. 2(a) and (b) showed that T_D was noticeably shorter than the surrounding periods of the oscillatory intervals, and this effect appears more pronounced in the 2 Hz condition. Does this reflect a constant movement time for the given shift in joint angle position or is an effect of the rhythmic movement detectable? A mixed-design 2 (movement direction) \times 2 (oscillation frequency) \times 9 (participants) ANOVA was performed on T_D which yielded all three main effects significant. The major result is that T_D was significantly longer in trials performed at 2 Hz than at 3 Hz, $F(1, 72) = 72.74$, $p < 0.0001$. Flexion was significantly shorter than extension, $F(1, 72) = 7.57$, $p < 0.001$: 2 Hz: 377 ms (Flexion), 396 ms (Extension); 3 Hz: 301 ms (Flexion), 334 ms (Extension). The main effect of participants was significant, $F(8, 72) = 4.20$, $p < 0.001$, and a three-way interaction was also significant, $F(8, 72) = 2.48$, $p < 0.05$. All participants' data are plotted in Fig. 3. Despite their differences, they all display the same pattern of increasing T_D across the two oscillation frequencies.

An additional test was performed to discern whether the discrete movement is modified by the pre- and succeeding oscillation. When peak velocity was submitted to the same ANOVA as above, the results revealed a similar pattern as observed for T_D . There was a main effect for frequency: $F(1, 72) = 87.83$, $p < 0.0001$, a main effect for participants: $F(1, 72) = 37.55$, $p < 0.0001$, and a two-way interaction between movement direction and participants, $F(8, 72) = 3.88$, $p < 0.001$. The overall means of peak velocities in the two frequency conditions were: 2 Hz: 298°/s; 3 Hz: 349°/s.

3.4. Influence of the rhythmic onto the discrete movement: onset of the discrete movement

An important indicator for determining whether the ongoing oscillation has an effect on the discrete movement is the onset of the discrete movement.

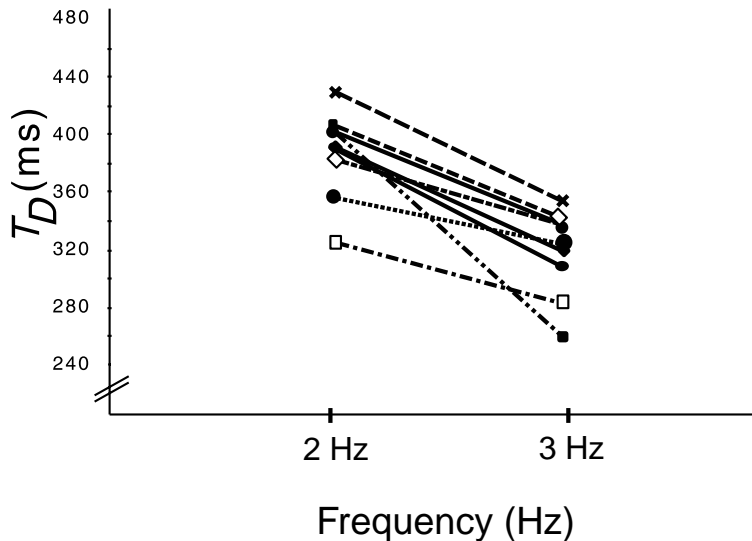


Fig. 3. The durations of the discrete movements T_D in the two frequency conditions shown for all nine participants.

If only the phase of the trigger signal and reaction time determines the initiation of the discrete movement, then the discrete movement should start at random phases in the ongoing oscillation, because the metronome signal was triggered at random phases. The phase of the discrete movement's onset ϕ was determined in two ways. On the basis of the super-threshold EMG activity ϕ was calculated by either using the periods of the EMG signal, ϕ_{EMG} , or the phase of the joint angular signal, ϕ_{angle} . Fig. 4(a) displays a polar histogram of the ϕ_{angle} for four exemplary participants. None of the participants showed any noteworthy differences between the four different conditions and the figure clearly identifies a unimodal distribution with a mode around $\pi/2$ rad. This phase lies in the trajectory segment traversing in opposite direction to the discrete movement (see Fig. 1). Using ϕ_{EMG} the histogram of four participants is displayed in Fig. 4(b). A slightly broader distribution can be seen with its mode between $3\pi/2$ and 2π rad. This shows that the discrete movement's onset occurs shortly before the rhythmic burst would have occurred if the oscillation had been continued. Fig. 4(c) and (d) show ϕ_{angle} and ϕ_{EMG} pooled over all participants but separated for flexion and extension. The two conditions are clearly very similar. These results show that ϕ is tightly constrained by the ongoing rhythmic movement.

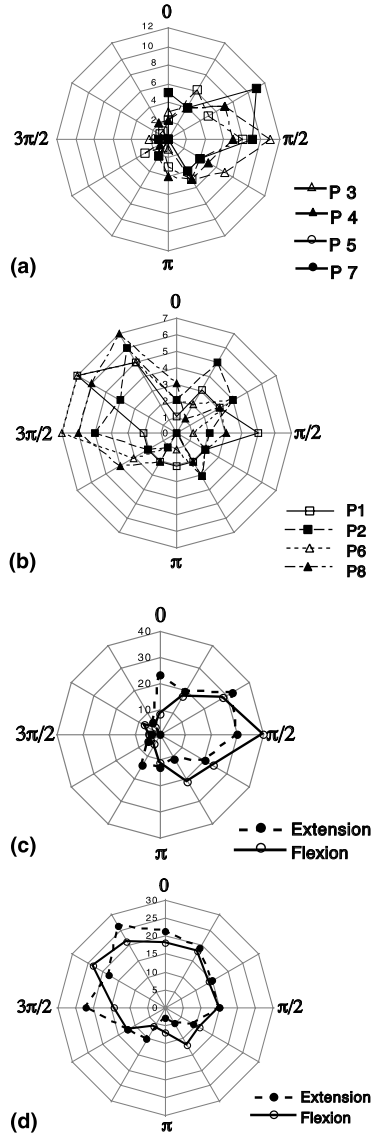


Fig. 4. Polar histograms show the distribution of the phase of the discrete movements' onset determined on the basis of the joint angle phase ϕ_{angle} or EMG phase ϕ_{EMG} . (a) ϕ_{angle} of four selected participants; (b) ϕ_{EMG} of four selected participants; (c) ϕ_{angle} pooled over all participants showing flexion and extension trials separately; (d) ϕ_{EMG} pooled over all participants showing flexion and extension trials separately.

3.5. Effect of the discrete onto the rhythmic movement: Phase resetting and Phase shift

The preceding analyses of the kinematic parameters in the pre- and post-discrete intervals established that the oscillation was marginally but systematically affected. Another typical parameter to evaluate the nature of the perturbation on an ongoing oscillation is its shift in phase. While the signature of a forced or paced oscillator is that the oscillation returns to its original phase entrainment with the forcing oscillator, an autonomous oscillator is typically shifted by the perturbation by some amount (Winfree, 1990). For a quantitative evaluation of this phase resetting $\Delta\phi$ was calculated for each trial. Fig. 5(A) and (B) show the frequency distribution of $\Delta\phi$ in all 3 and 2 Hz trials separately while pooling over all participants. The 3 Hz condition clearly shows a unimodal distribution with a mode around 1 rad, which may be close enough to speak of a $\pi/4$ rad shift. The majority of trials showed a phase delay, indicating that the trial segment with the discrete movement is longer than a cycle. The fewer trials with a negative value of $\Delta\phi$ indicate a phase advance. In the 2 Hz condition two modes appear which are around -1 and $+1$ rad or, tentatively, $-\pi/4$ and $+\pi/4$ rad. There are more trials that show a phase advance. The observation of a phase shift speaks to a perturbing influence of the discrete onto the rhythmic component.

A 2 (oscillation frequency) $\times 2$ (movement direction) $\times 9$ (participants) ANOVA was conducted on $\Delta\phi$ to find out whether the experimental conditions had a marked effect on the phase shift. All three main effects were significant: oscillation frequency: $F(1, 72) = 33.75$, $p < 0.0001$; movement direction: $F(1, 72) = 44.64$, $p < 0.0001$; participants: $F(1, 72) = 12.55$, $p < 0.0001$. The differences among participants are of no further concern in this context and no interaction effects are observed with participants. The differences in oscillation frequency showed a significant interaction, $F(1, 72) = 6.08$, $p < 0.05$: The mean values identify that flexion trials had a longer $\Delta\phi$ than extension trials, and the 3 Hz conditions showed more phase delay than the slower 2 Hz condition: 2 Hz: 0.07 rad (flexion), 0.65 rad (extension); 3 Hz: 0.50 rad (flexion), 1.68 rad (extension). As T_D was already shown to be longer in extension than in flexion trials, these results reveal that $\Delta\phi$ in the rhythmic pattern was determined by the relative speed of the oscillatory movement and the duration of the discrete movement.

Given the systematic effects in $\Delta\phi$ one further inquiry typically undertaken in phase resetting studies seeks to determine whether $\Delta\phi$ is a function of the onset phase of the perturbing event. In the present scenario we asked whether

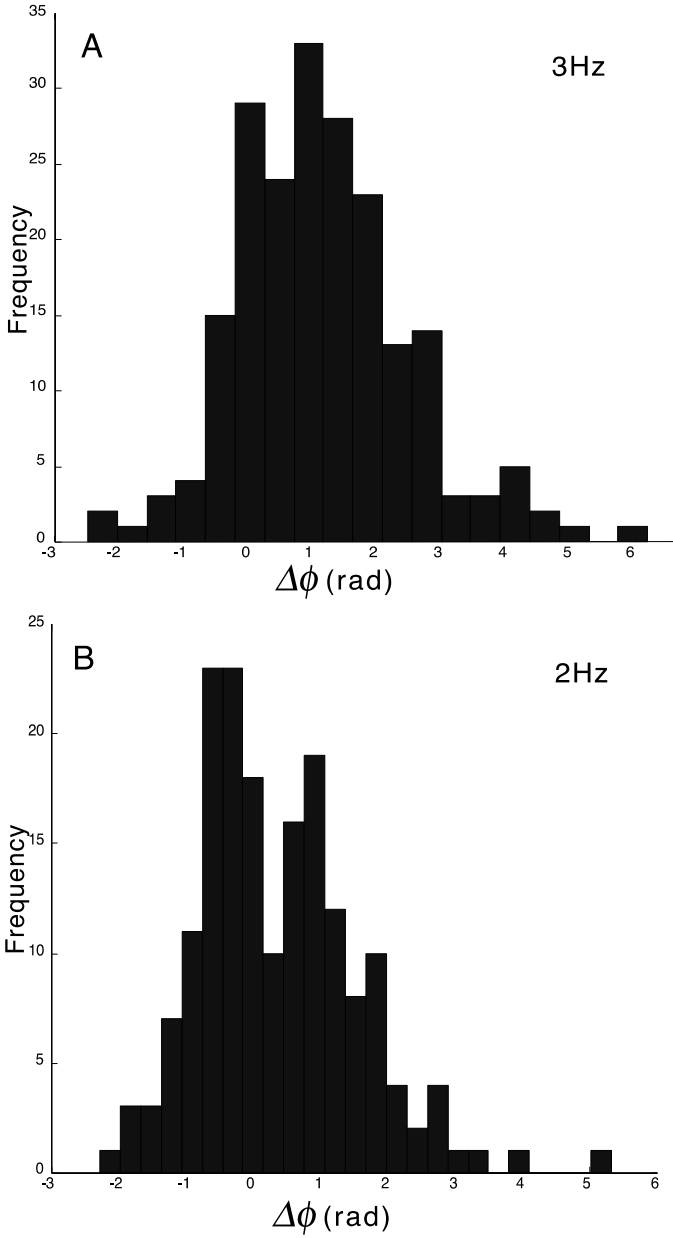


Fig. 5. Histogram of the phase shift of the oscillation $\Delta\phi$ for the 3 Hz condition (A) and the 2 Hz condition (B).

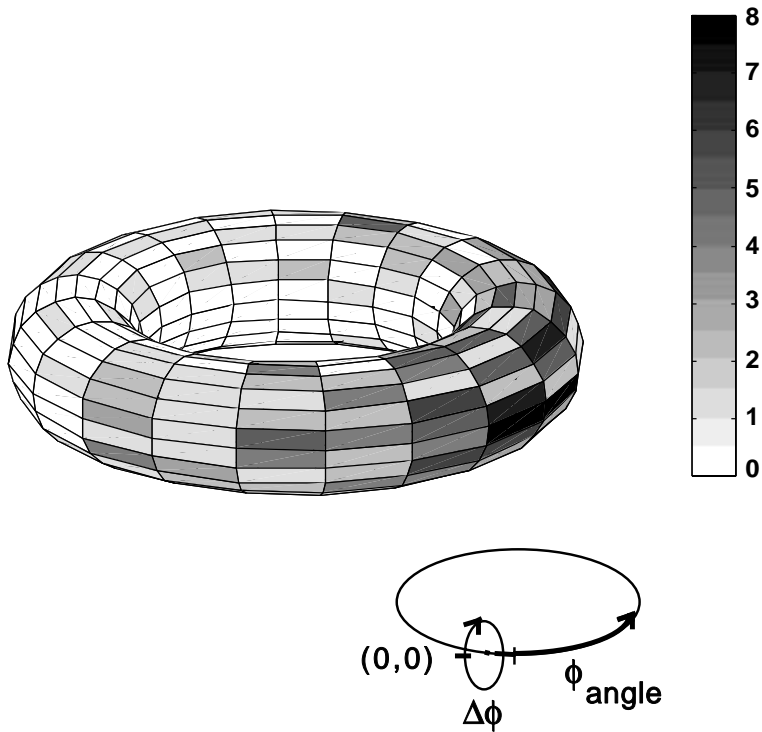


Fig. 6. Histogram correlating the phase shift of the oscillation $\Delta\phi$ with the onset of the discrete movement ϕ_{angle} . ϕ_{angle} is plotted around the larger circle where zero is defined at the front as indicated on the inset. $\Delta\phi$ is plotted on the inner circle where zero is defined as indicated on the inset. Darker shading reflects higher frequency of occurrence.

$\Delta\phi$ was a function of ϕ_{angle} and of ϕ of the metronome. While correlations of $\Delta\phi$ with the phase of the metronome did not show any systematic dependencies, Fig. 6 displays the relation between $\Delta\phi$ and ϕ_{angle} . The torus shows a histogram of $\Delta\phi$, plotted on the large circle, against ϕ_{angle} , plotted on the small circle. The most frequent occurrences, in the shape of a unimodal distribution and indicated by darker shading, were found where $\Delta\phi$ was between 0 and $\pi/4$ rad whenever ϕ_{angle} is $\pi/2$ rad. The torus is so oriented that only very few events are hidden underneath or behind the torus.

3.5.1. Reaction time

As one other parameter of the data analysis premotor reaction time was determined. The mode of the asymmetric distribution was found at 240 ms with participants' means ranging from 194 to 396 ms. Individual trial values

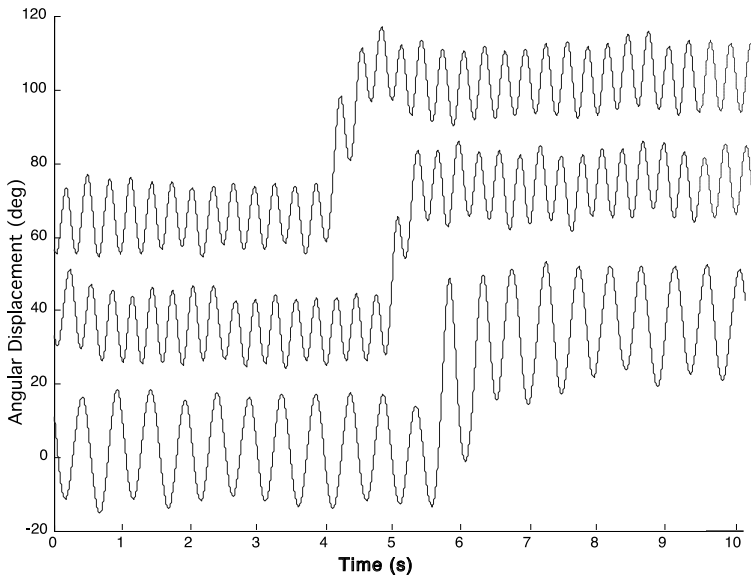


Fig. 7. Time series where rhythmic and discrete movements co-occur. The scale of the y -axis shows degrees, but the center of oscillation of each trial is offset in order to present the three trials together in one figure.

ranged from a minimum of 100 ms to a maximum of 600 ms. The large range is probably due to the fact that the instruction emphasized a fast change in joint angle as well as a fast onset of the discrete movement. Reaction time did not show any dependency on the onset phase of the metronome stimulus.

3.5.2. Trials with co-occurring discrete and oscillatory movements

In approximately 8% of the trials, the instruction to shift target *without stopping* the oscillatory motion, lead to a superposition of oscillations onto the discrete movement. Fig. 7 shows three of such trials, revealing that the oscillatory and the discrete movements were sometimes not entirely separated and the shift in the center of oscillation was still continuing although oscillations occur. To further elucidate this event ϕ_{angle} was determined for these trials. While there was no particular ϕ_{angle} preferred, none of these trials showed the typical ϕ_{angle} of $\pi/2$ rad.

4. Discussion

Almost all movements as they occur in daily life consist of rhythmic and translatory components, either concatenated into a sequence or happening

simultaneously. Rhythmic and translatory movements can be performed by different effectors or merged in the movements of one articulator or degree of freedom. A straightforward example is the action of cleaning a table where the usually cyclic wiping actions of the hand around the wrist or elbow joint are combined with a translation of the hand and arm across the table surface. Gestures in speech production, such as the opening and closing of the lips, occur rhythmically but are continuously modulated with protrusion, retraction, or rounding of the lips to shape the air flow for different vowels and consonants. While rhythmic components are the repeated movements around one axis of rotation, usually coincident with the joint axis, discrete components refer to the displacement of the effector and the midpoint of oscillation from one point in external space to another. The hypothesis pursued in this study is that natural movements can be decomposed into such discrete and rhythmic elements. These two types of behaviors are assumed to form two movement primitives underlying the generation of more complex behavioral actions or action sequences. The often complex trajectories observed at the endpoint of an effector are understood as the result of a merging of these movement primitives. In a previous study, Sternad and Schaal (1999) scrutinized the issue of segmentation of endpoint trajectories in the task of drawing of a figure-eight pattern in 3D. The authors showed that the apparent discontinuities and the piecewise planarity in the three-dimensional endpoint kinematics that suggested a segmentation in the control were in fact spurious effects. The same trajectories could be produced by continuous rhythmic movements in the joint degrees of freedom of the arm. Rhythmic primitives in the seven biomechanical degrees of freedom of the arm could account for the observed planarity in conjunction with effects of the biokinematic chain and the nonlinear transformation from joint space into Cartesian space. In the same spirit, Schaal and Sternad (2001) demonstrated that the $2/3$ power law observed at the endeffector trajectory arises from oscillatory patterns in joint space.

The hypothesis that discrete and rhythmic elements may be two movement primitives is motivated by the fact that point attractor and limit cycle attractor dynamics are the two primary stable regimes of a nonlinear dynamic system. Numerous studies have already shown that rhythmic actions can be successfully modeled as the stable performance of nonlinear oscillations, typically using models of second-order dynamics with nonlinear terms. This was demonstrated for a single degree-of-freedom system (Beek, Rikkert & van Wieringen, 1996; Kay, Kelso, Saltzman & Schönner, 1987), for two degrees of freedom as in bimanual coordination (Grossberg, Pribe & Cohen,

1997; Haken, Kelso & Bunz, 1985; Sternad, Amazeen & Turvey, 1996) or for chains and networks of oscillations (Cohen, Holmes & Rand, 1982; Kopell, 1993; Collins & Richmond, 1994). The understanding that discrete actions may be governed by an equilibrium point dynamics has been promoted by the equilibrium-point hypothesis (Abend, Bizzi & Morasso, 1982; Feldman, 1986; Gribble & Ostry, 1996; Latash, 1993). In continuation of these two strands of work, the present study explores whether these two regimes can be understood as fundamental movement patterns constituent in forming more complex actions and action sequences. The level of analysis chosen here is the level of the biomechanical joint degrees of freedom. Note, though, that we make no claims about the exclusive or primary importance of this level of analysis, rather that these two stable regimes are predominant structures of organization on any level of analysis.

If two stable regimes are fundamental in shaping the movement output, the question is how do they co-exist or interact. Investigating a single degree-of-freedom task that combined rhythmic and discrete movement components, Adamovich et al. (1994) empirically addressed the question whether discrete and rhythmic control signals can co-occur, or whether they have to be issued in sequence. On the basis of detailed kinematic analyses of the forearm trajectories, the authors concluded that the control signals have to be sequenced at the central level and a merging of the features occurs at the periphery. We propose a model in which the rhythmic and discrete pattern generators are coupled by mutual inhibition such that they produce the observed interaction and sequencing effects. To obtain a detailed set of data as guideline for the modeling we performed an experiment similar to the one by Adamovich et al. (1994). The experimental task consisted of a single-degree-of-freedom elbow movement in which participants were instructed to oscillate their forearm at a prescribed frequency and to switch the midpoint of oscillation to a second target after triggering by an auditory signal. Participants were instructed to perform both aspects of the task simultaneously. The difference to the experimental task of Adamovitch et al. was that the oscillation frequencies were precisely controlled by a metronome and were set to either 2 or 3 Hz, instead of the high frequencies of 5–7 Hz that Adamovitch et al. chose. The reason for our choice was that we preferred frequencies that were close to volitional rhythmic movements.

Analyses of kinematic and electromyographic data aimed to extricate mutual effects of the rhythmic and the discrete components onto each other. The experimental results corroborated and further detailed the findings of the literature. Comparison of the average periods and amplitudes of the

oscillations before and after the discrete movement verified that the oscillation was only marginally affected by the transition. The transients in both periods and amplitudes after the discrete transition were relatively short and the observed under- or overshoot of the post-discrete amplitude only lasted one cycle. Both of these findings suggest that the initial oscillation was only slightly perturbed – possibly by a transient increase of co-contraction after the discrete movement. This interpretation would speak more to a perturbation than a cessation of the oscillatory signal during the discrete movement, as would be the case if the rhythmic and discrete signals were issued in strict sequence. If the oscillatory signal were temporarily terminated, a more marked transient to the previous frequency/amplitude relationship would be expected.

Further, the duration of the discrete movement was significantly shorter than the oscillatory period in both frequency conditions, but comparison of the discrete movement's duration in the two frequency conditions showed that T_D was significantly longer in the slower oscillation condition. Concomitantly, peak velocity of the discrete movement was higher in trials with a faster oscillation. This result is in contrast to Adamovich et al.'s findings which, after subtraction of the oscillatory parts of the total signal, showed no evidence for any influence of the rhythmic onto the discrete movement. This result was one of the cornerstones in their argument that the task was controlled centrally as a sequence of rhythmic and discrete control signals. While our results do not exclude the possibility that these merging effects occur at the peripheral level, they do not contradict the hypothesis that parallel activation at a central level is possible and they take the stringency out of Adamovich et al.'s conclusion.

In corroboration of previous results of the literature on tremor and volitional movements, the onset of the discrete action is confined to a small phase window of the ongoing oscillation. This calculation of ϕ was performed by using both the EMG bursts and the kinematic peaks as reference frames for determining ϕ of the discrete movement. Using EMG bursts as the reference frame, the distribution of ϕ_{EMG} showed that the super-threshold bursts, initiating the discrete shift of the oscillation midpoint, occurred during the last quarter of the cycle, approximately $\pi/4$ rad before the rhythmic burst would have occurred. This result replicates the results of Adamovich et al. despite the considerable difference in oscillation frequencies. In addition to their analyses, ϕ was also calculated against the running phase of the kinematic oscillation. Due to the phase difference between EMG and kinematic landmarks, the mode of the histogram of ϕ_{angle} was at $\pi/2$ rad. In this phase

segment the trajectory is directed away from the direction of the discrete transition. This contrasts with Goodman and Kelso's (1983) results where the discrete volitional movement appeared to utilize, rather than run counter the momentum of the ongoing rhythmic movement. The reason for this difference may lie in the fact that these authors calculated ϕ with very conservative criteria. Yet, it may also be due to the fact that EMG and kinematic data have different phase relations depending on the frequency of oscillation (see Elble et al., 1994).

The only analysis that does not reveal any influence from rhythmic onto the discrete movement is the one on premotor reaction time. Contrary to the literature (Latash, 2000; Staude et al., 1995) we found no modulation of premotor reaction time as a function of the phase of the ongoing oscillation. This speaks to the fact that the latency interval prior to observed myographic activity is not systematically affected by the ongoing rhythmic movement. This absence of effect is difficult to understand given the unimodal distribution of ϕ_{EMG} . This incongruence of effects must be due to additional changes in the relation between the kinematic and the electromyographic signals that make ϕ values more constrained than simple RT values.

Further detailing Adamovich et al.'s qualitative observation that phase resetting occurs, we calculated phase shifts $\Delta\phi$. For the 3 Hz condition a unimodal distribution was observed with 1 rad, or approximately $\pi/4$ rad, as the predominant $\Delta\phi$ value. In very few cases a phase advance was observed. For the 2 Hz condition there was a bimodal distribution with peaks at $\Delta\phi = -\pi/4$ rad and $+\pi/4$ rad, showing approximately as many phase advances as phase delays. $\Delta\phi$ was a unimodal function of ϕ , as shown in Fig. 6. In Adamovich et al.'s line of argument, a non-zero $\Delta\phi$ was interpreted as an interruption of the oscillation. While this is possible in principle, phase resetting is also a typical phenomenon indicative of an ongoing autonomous nonlinear oscillation, in contrast to a forced oscillation which does not show phase resetting (Winfree, 1990). Therefore, the interpretation that an oscillatory control signal does not co-exist with a discrete control signal is not stringent. We propose that both units can be active simultaneously but that they inhibit each other during certain phases of the oscillation. It is this inhibition that gives rise to the sequentiation of the two action components.

The one observation in our data that directly supports our argument that the oscillatory and translatory control signals are activated in parallel is demonstrated in Fig. 7. A small set of trials (8%) revealed that oscillations can indeed co-occur with the discrete movement. This can only be understood by assuming that the oscillation is suppressed or inhibited during the

discrete movement, but not entirely aborted. It should be noted, though, that in these trials the onset of the discrete movement occurred at atypical phases of the oscillation. This obviously led to an atypical “mixing” or lack of suppression of the rhythmic movement. This observation is important, because, as mentioned before, there are many tasks in which simultaneous discrete and rhythmic actions are necessary and, in principle, some mechanism must be conceived. One reason why Adamovich et al. may not have observed such merging effects is that they used frequencies much faster than the 2 and 3 Hz frequencies in the present study. It is conceivable that the lack of suppression of the rhythmic component becomes more probable for slower movements.

On the basis of these data we proceed to develop a model of two pattern generators with mutual inhibitory coupling.

4.1. Modeling discrete and rhythmic pattern generators

To capture the data of our experiment, two kinds of movement generating mechanisms are needed, one for discrete and one for rhythmic movements. Since the focus of our investigations lies on capturing the reciprocal influence of discrete and rhythmic movements, a model based on differential equations is the natural choice since such systems allow to incorporate this mutual influence through coupling terms. The modeling strategy is most closely related to methods developed for pattern generators (PG), and it inherits a similar degree of biological realism and abstraction (Kopell, 1993; Rall, 1995; Softky & Koch, 1995).

We propose that each degree of freedom of a joint is described by two variables, a rest position θ_0 and a superimposed oscillatory position, θ_R as sketched in Fig. 8. By changing θ_0 from an initial to a target position, discrete motion is generated. Rhythmic movement θ_R is produced by oscillations around the rest position θ_0 . Rhythmic and discrete actions can be generated by a combination of an oscillatory motion and a change in the rest position. Some elements of this modeling framework have already been shown to account for multiple-link effector movements and were used in artificial movement control (Schaal & Sternad, 1998).

4.2. The rhythmic pattern generator

The equations for the rhythmic PG are inspired by the half-centered oscillator model (Brown, 1914). The central notion of this model is that two

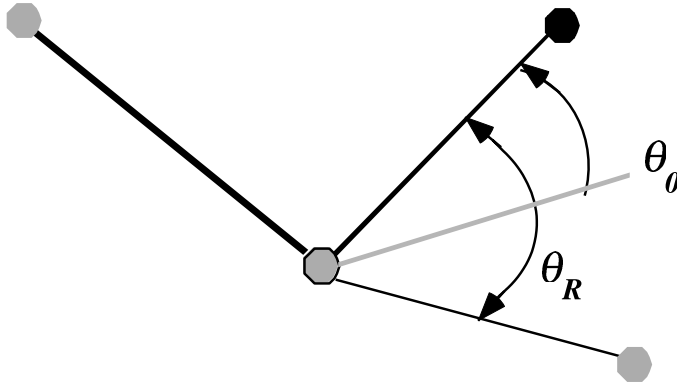


Fig. 8. Each degree of freedom of a limb has a rest state θ_0 and an oscillatory state θ_R . Discrete movements are defined as changes in the rest state θ_0 , oscillations are defined as rhythmic movements θ_R around θ_0 .

neurons mutually inhibit each other, while they are both individually excited by a tonic stimulation and thereby alternate in producing a burst of activity (see Fig. 9).

Matsuoka (1985, 1987) formulated this neurophysiological concept into a set of leaky integrator equations:

$$\begin{aligned}
 T_1 \dot{\psi}_i &= -\psi_i + s - b\zeta_i - w[\psi_j]^+, \\
 T_2 \dot{\zeta}_i &= -\zeta_i + [\psi_i]^+,
 \end{aligned}
 \tag{1}$$

ψ_i is the state variable for the unit i which is tonically excited by s and is interpreted as the mean firing rate of a neuron. The symbol $[.]^+$ denotes a threshold function that sets negative values to 0 while not affecting positive values, thus simulating the fact that physiological neurons do not have negative firing rates. The threshold is the only nonlinearity in the model. An important feature introduced by Matsuoka is the adaptation parameter ζ_i which modulates the decay time of ψ_i close to what is observed in biological

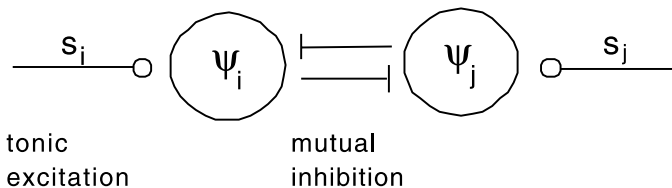


Fig. 9. Schematic depiction of a half-center oscillator.

neurons. ζ_i , is itself is governed by a leaky integrator equation. T_1 and T_2 are two time constants for the output ψ_i and the adaptation ζ_i , respectively. Important in these equations is the inhibitory coupling from the antagonistic unit ψ_j . Matsuoka (1985, 1987) demonstrated the stability properties of these neural oscillators in pairs, rings and larger networks.

For the present purpose of modeling macroscopic movement kinematics, this model is interpreted to represent the activity of a neuronal ensemble that leads to the innervation of one muscle or muscle group. The two mutually opposing neuronal ensembles are therefore likened to the cooperation of two antagonistic muscles or synergies. With this level of analysis in mind, some further modifications are introduced:

$$\Delta p_i = [A - \theta_{R,i}]^+, \quad (2)$$

$$\dot{\xi}_i = -a_\xi(\xi_i - \Delta p_i),$$

$$\dot{\psi}_i = (-a_\psi \psi_i + b \xi_i - d \zeta_i - w[\psi_j]^+) c_R, \quad (3)$$

$$\dot{\zeta}_i = (-a_\zeta \zeta_i + [\psi_i]^+) c_R,$$

$$\dot{\theta}_{R,i} = [\psi_i]^+ - [\psi_j]^+. \quad (4)$$

Eqs. (2) describe the excitation where A is the desired amplitude, and the difference between the current position θ_R and the desired amplitude Δp_i produces a time-varying excitation. After passing this initial step function through a low-pass filter, ξ_i becomes the excitatory input, corresponding to s in the original model. This position-dependent excitation ensures that the oscillation remains centered around the rest position which is set to zero. Eqs. (3) are the original equations suggested by Matsuoka (1985, 1987). The frequency of the oscillator is entirely determined by the parameter c_R , capturing the effect of the time constants T_1 and T_2 above, which modulates both ψ_i and ζ_i . Finally, the continuous oscillatory signal $\theta_{R,i}$ is obtained by subtraction of the positive parts of the two units i and j , i.e., by adding the agonistic and antagonistic component.

One further important change is that the output is interpreted as a velocity signal. This is motivated by recent findings in brain imaging studies where close correspondence was found between the velocity and neuronal activity (Ebner, 1998; Ebner & Fu, 1997; Kelso, Fuchs & Jirsa, 1999). A more technical argument for this choice is that this modification ensures that the rhythmic movement amplitude decreases with increasing frequency – position coding does not capture this effect. Therefore, Eq. (4) is an integrator to

determine the angular position $\theta_{R,i}$ of the oscillator. Despite these favoring arguments, it should be pointed out that this mapping between a velocity output from a neuronally inspired model and the actual movement velocity sidesteps the issue of the dynamics of the executing limb. We recognize that neuronal structures probably do not directly specify external variables describing motor output, such as position, torque, EMG level, stiffness. Rather, central structure determine system parameters, which, in turn, influence the output variables. Yet, we see our modeling as a first promising step which combines dynamical modeling of observable behavior with the level of an abstracted neuronal substructure.

Fig. 10 shows position and velocity of the oscillatory movement for three different parameter combinations of c_R and A . The bottom trace displays the velocity bursts alternately produced by each of the two units. The upper trace shows the continuous integrated position signal. Frequency is entirely modulated by c_R , and also affects the amplitude A . Conversely, when A is modulated, the actual amplitude changes without affecting frequency. It should also be noted how quickly frequency and amplitudes change to a new

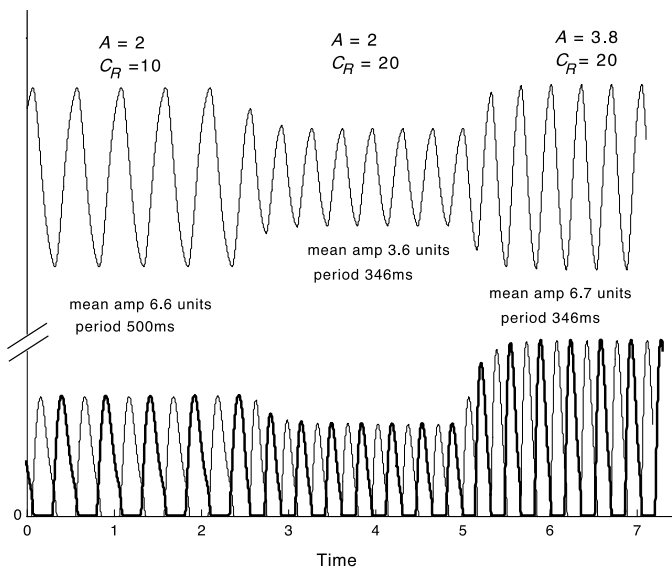


Fig. 10. Position and velocity trajectories of the rhythmic pattern generator with three parameter combinations c_R and A as shown. Changes in A do not affect the movement frequency, but changes in c_R have an effect on movement amplitude. The other parameter values are: $w = 2$, $a_\xi = 50$, $a_\psi = 1$, $b = 20$, $d = 1$, $a_\zeta = 5$.

steady state value, i.e., that the transients are rather short as observed in human movement.

4.3. The discrete pattern generator

Discrete movement is generated by a set of weakly nonlinear differential equations, closely related to the VITE model by Bullock and Grossberg (1988, 1991). The modeling strategy is again to use first-order differential equations, i.e., leaky integrators, as basis for the development – similar to models of biological neurons. These equations are augmented with nonlinear terms such that an attractor landscape is created that produces smooth trajectory profiles between initial and target states. In contrast to VITE, this dynamical system does not require artificial resetting of certain states of the attractor model after each movement, as all states of the dynamical system converge to their initial states after the movement terminates (see discussion in special issue Bullock & Grossberg, 1991). The following equations represent the discrete pattern generator for one antagonistically actuated degree-of-freedom joint, where i and j indicate the agonist and antagonist unit:

$$\begin{aligned}\Delta v_i &= [T_i - \theta_{0,i}]^+, \\ \dot{v}_i &= a_v(-v_i + \Delta v_i),\end{aligned}\tag{5}$$

$$\begin{aligned}\dot{x}_i &= -a_x x_i + (v_i - x_i)c_D, \\ \dot{r}_i &= a_r(-r_i + (1 - r_i)ev_i), \\ \dot{z}_i &= -a_z z_i(x_i - z_i)(1 - r_i)c_D,\end{aligned}\tag{6}$$

$$\dot{\theta}_{0,i} = a([z_i]^+ - [z_j]^+)c_D.\tag{7}$$

The goal of the discrete PG is to produce a velocity trajectory z_i with an approximately symmetric bell-shaped velocity profile, similar to those observed in humans (e.g., Hogan, 1984). In correspondence to Eqs. (2) for the rhythmic PG, Eqs. (5) build a difference vector Δv between the target position T_i and the current position θ_i of each unit and pass this difference vector through a first-order differential equation. While v_i resembles a signal observed in the primate cortex (Bullock & Grossberg, 1988, 1991), the two variables x_i and r_i in Eqs. (6) are intermediate variables that accomplish a smoothing of v_i and a nonlinear gain amplification to approximate the bell-shaped velocity profile. In correspondence to c_R in the rhythmic PG, c_D adjusts the speed and duration of the movement.

Eq. (7) yields the subtracted value of both units, analogous to Eq. (4), to be interpreted as the velocity signal z_i of the joint. For simplification, we assume that the current position and target of each muscle are identical but only of the opposite sign. Fig. 11 illustrates how the burst-like signals v_i , x_i , and r_i change towards an increasingly symmetric bell-shaped signal z_i and the integrated position output θ_0 .

Note that these signals should not to be equated with electromyographic signals. While in the model a step change in the target parameter initiates the burst that gets shaped toward the bell-shape velocity curve, EMG bursts during discrete movements display the typical triphasic burst pattern. Research from the equilibrium point hypothesis has shown that the basic control signal underlying discrete movements (the shift in the equilibrium state) ceases to change before peak velocity (Feldman, Adamovich & Levin, 1995).

4.4. Interaction of discrete and rhythmic pattern generator

In order to address the question of the interaction of the discrete and rhythmic unit, the two units are coupled. The primary result in our data and the literature is that the discrete movement's onset is confined to a small

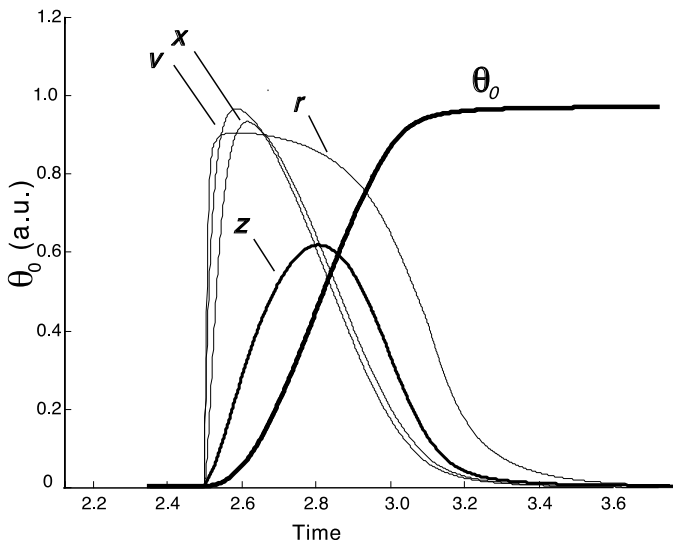


Fig. 11. Time course of intermediate variables v, x, z and r of Eqs. (5) and (6) and output variable θ_0 of Eq. (7) of the discrete pattern generator. The parameter values of the equations are: $T_i = -2$, $a_v = 50$, $a_x = 1$, $a_r = 50$, $e = 10$, $a_z = 0.01$, $a = 0.08$.

phase window of the rhythmic movement. To capture this effect, the two PGs are cross-coupled via the central parameters c_D and c_R :

$$\begin{aligned}\dot{c}_{D,i} &= -\alpha_D(c_D - c_{D,\text{set}}) - w_D[\dot{\psi}_j]^+, \\ \dot{c}_{R,i} &= -\alpha_R(c_R - c_{R,\text{set}}) - w_R[\dot{z}_j]^+.\end{aligned}\quad (8)$$

The value of the frequency parameter c_D of the discrete unit i changes as a function of the rhythmic activity ψ of unit j , weighted by w_D , and returns to a set value $c_{D,\text{set}}$, scaled by α_D . To illustrate this interaction the experimental elbow joint movement is used: When the biceps (i) performs a flexion contraction during the oscillatory movement with positive acceleration, the antagonistic triceps activity (j) is inhibited by a decrease in $c_{D,i}$ and therefore temporarily inhibits a discrete elbow extension. Conversely, when the discrete unit's activity in j (triceps) is active and is positively accelerating, it suppresses the rhythmic activity in i (biceps). The phasing of this inhibition is modulated by the magnitude of $\dot{\psi}$ and the relative weights of α and w . This cross-coupling was used in all of the following simulations and analyses. It is conceivable that such a coupling is implemented by spinal interneuronal circuitry.

4.5. Modeling the experimental results

To model the experimental results simulations were run with a set of 150 randomly timed step changes in the discrete target T_i . All other parameters in rhythmic and discrete PG and the cross-coupling were fixed. Subsequently, the simulated trajectories were submitted to analyses corresponding to the ones performed on the experimental data. Fig. 12 shows three time series of simulated data with three different onset times for the target shift T_i . All parameter values are listed in the figure caption. The onset of the T_i shift is indicated by the thick vertical bars. The exemplary trajectories show the relatively short transient after the discrete movement back to the frequency and amplitude values of the original oscillation. Both under- and overshoots at A_1 were obtained. The bottom trial shows the intrusion of oscillations during the discrete transition as observed in the data. This occurred in approximately 5% of the simulation runs in which the onset of the discrete target T_i shift fell into in a small phase window where the acceleration of the antagonistic units was positive and small. As a consequence, the inhibition of the discrete agonistic unit is small so that the discrete movement can be initiated. Yet, the rhythmic unit is still active and competes with the discrete unit. It is this type of interaction that can account for both the apparent

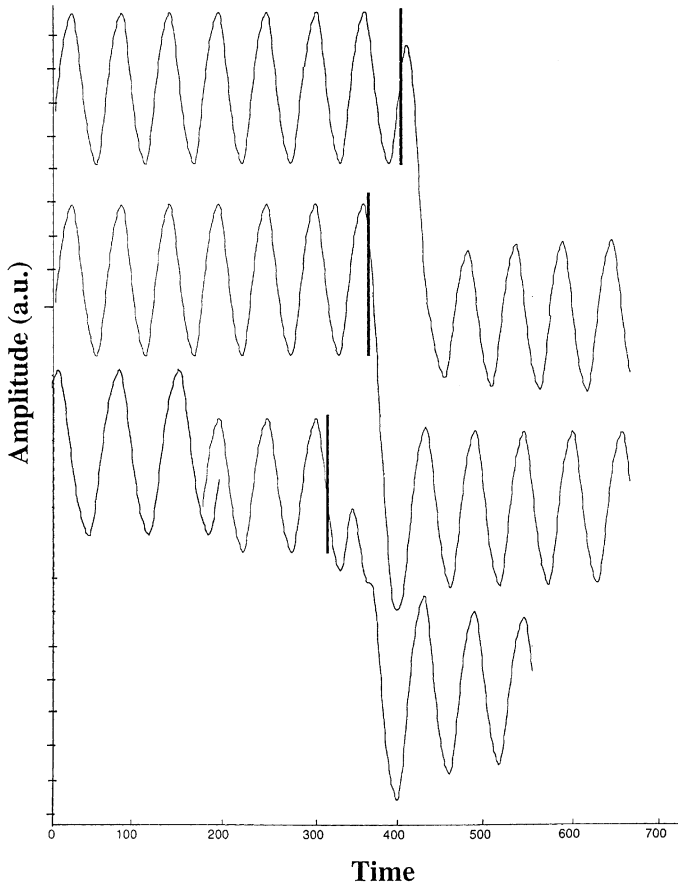


Fig. 12. Three representative trials of the simulated position trajectory of the coupled system. The vertical bars indicate the onset of the step change in T_i whose phase is different for the three trajectories. The trajectory at the bottom exemplifies a trial with an inserted oscillation during the discrete transition. The parameter values for the pattern generators and the coupling are the same as before. The coupling parameters are: $c_{D,set} = 150$; $c_D = 80$; $\alpha_D = 50$; $c_{R,set} = 10$; $c_R = 20$; $\alpha_R = 20$.

sequencing and the co-occurrence of rhythmic and discrete movements observed in the human data. One difference between the model and the data, though, is that the phase window in the model is relatively short, whereas in the human data such co-occurrences were found at many different phases of the discrete movement's onset.

The next focus was directed to the onset phase ϕ of the discrete movement. As no EMG data are available, the onset ϕ was calculated from the velocity

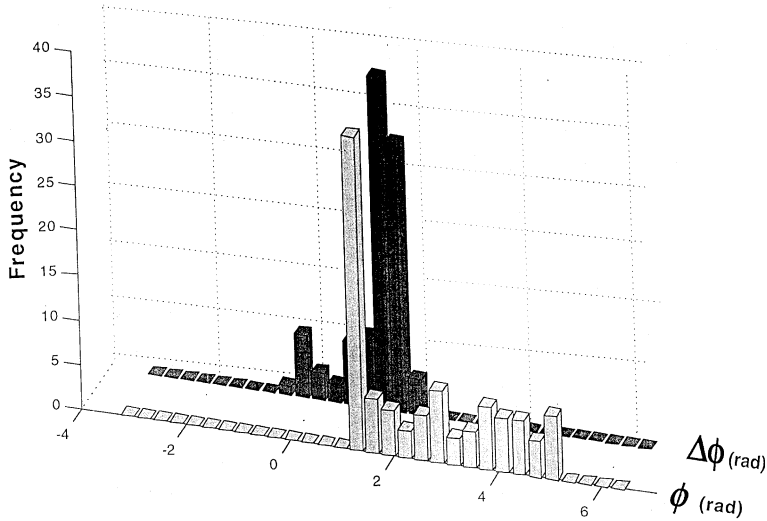


Fig. 13. Histograms of ϕ and $\Delta\phi$ calculated from the simulated data.

signal of the discrete PG ψ . The threshold for the onset ϕ was set to 5% of the maximum velocity during the transition. Fig. 13 shows the histogram of ϕ in the front panel. It highlights that ϕ is confined to a limited window of phases with a peak close to 1 rad, or $\pi/2$ rad as seen in the human data. The marked peak close to 1 rad is the result of the inhibition of discrete movements in the preceding phase window where discrete movements are inhibited. The histogram in the second panel of Fig. 13 shows the phase shifts $\Delta\phi$ extracted from the same set of simulated data. As in the human data there is a unimodal peak close to 1 rad, while fewer instances of are found between -1 and 1.5 rad. Note, as in the human data, positive and negative $\Delta\phi$ are observed.

5. Conclusions

This study tested the hypothesis that human limb movements can be captured in terms of two fundamental units of action described as two stable dynamical regimes for discrete and rhythmic movements. For rhythmic movements we suggested an oscillatory pattern generator, modeled in the spirit of half-center models of neurons. For discrete movements we developed a point attractor dynamics following but modifying the modeling strategy of Bullock and Grossberg's VITE model. For each joint degree of freedom both

pattern generators can exist simultaneously but exert mutual inhibition onto each other. The suggested modeling framework provides a unified account for both discrete and rhythmic movements from a dynamical systems perspective on the basis of neuronal circuitry. As a test for this model we performed an experiment investigating human single-joint elbow movements involving both rhythmic and discrete movement elements. Motivated by Adamovitch et al.'s results, we reexamined their conclusions that rhythmic and discrete control signals have to be issued by the central nervous system in a sequence. Several empirical and modeling results showed that the apparent sequencing can be accounted for by a co-existence and inhibitory interaction of rhythmic and discrete control signals. The empirical finding giving rise to our hypothesis of inhibitorily coupled discrete and rhythmic control signals is the occasional intrusion of oscillations during the discrete movement. As further support for this hypothesis, the model of two pattern generators was developed. Simulation results demonstrated that the effects observed in human performance can be replicated using the two pattern generators with a mutually inhibiting coupling. In ongoing work this modeling framework is further developed to address multi-joint coordination in human and robot systems.

Acknowledgements

This research was supported by the NSF Research Grant SBR 97-10312. A short poster version of this study was presented at the 10th International Conference for Perception and Action in Edinburgh, Scotland, August 1999. We would like to thank Anatol Feldman for his very helpful comments.

References

- Abend, W., Bizzi, E. & Morasso, P. (1982). Human arm trajectory formation. *Brain*, *105*, 331–348.
- Adamovich, S. V., Levin, M. F. & Feldman, A. G. (1994). Merging different motor patterns: Coordination between rhythmical and discrete single-joint movements. *Experimental Brain Research*, *99* (2), 325–337.
- Beek, P. J., Rikkert, W. E. I & van Wieringen, P. C. W. (1996). Limit cycle properties of rhythmic forearm movements. *Journal of Experimental Psychology: Human Perception and Performance*, *22*, 1077–1093.
- Brown, T. G. (1914). On the nature of the fundamental activity of the nervous centers; together with an analysis of the conditioning of rhythmic activity in progression, and a theory of evolution of function in the nervous system. *Journal of Physiology*, *48*, 18–46.
- Bullock, D. & Grossberg, S. (1988). The VITE model: A neural command circuit for generating arm and articulated trajectories. In J. A. S. Kelso, A.J. Mandel & M. F. Shlesinger (Eds.), *Dynamic patterns in complex systems* (pp. 305–326). Singapore: World Scientific.

- Bullock, D. & Grossberg, S. (1991). Adaptive neural networks for control of movement trajectories invariant under speed and force rescaling. *Human Movement Science*, 10 (1), 3–55.
- Cohen, A. H., Holmes, J. & Rand, R. H. (1982). The nature of the coupling between segmental oscillators of the lamprey spinal generator for locomotion. A mathematical model. *Journal of Mathematical Biology*, 13, 345–369.
- Collins, J. J. & Richmond, S. A. (1994). Hard-wired central pattern generators for quadrupedal locomotion. *Biological Cybernetics*, 71, 375–385.
- Ebner, T. J. (1998). A role for the cerebellum in the control of limb movement velocity. *Current Opinion in Neurobiology*, 8 (6), 762–769.
- Ebner, T. J. & Fu, Q. (1997). What features of visually guided movements are encoded in the simple spike discharge of cerebellar Purkinje cells. *Progress in Brain Research*, 114, 431–447.
- Elble, R. J., Higgins, C. & Hughes, L. (1994). Essential tremor entrains rapid voluntary movements. *Experimental Neurology*, 126, 138–143.
- Feldman, A. G. (1986). Once more on the equilibrium point hypothesis (λ -model) for motor control. *Journal of Motor Behavior*, 18, 17–54.
- Feldman, A. G., Adamovich, S. V. & Levin, M. F. (1995). The relationship between control, kinematic and electromyographic variables in fast single-joint movements in human. *Experimental Brain Research*, 103, 440–450.
- Flash, T. & Hogan, N. (1985). The coordination of arm movements: An experimentally confirmed mathematical model. *Journal of Neuroscience*, 5 (7), 1688–1703.
- Goodman, D. & Kelso, J. A. S. (1983). Exploring the functional significance of physiological tremor: A biospectric approach. *Experimental Brain Research*, 49, 419–431.
- Goodwin, B. C. (1970). Biological stability. In C. H. Waddington (Ed.), *Towards theoretical biology*. Chicago, IL: Aldine.
- Gribble, P. L. & Ostry, D. J. (1996). Origins of the power law relation between movement velocity and curvature: Modeling the effects of muscle mechanics and limb dynamics. *Journal of Neurophysiology*, 76, 2853–2860.
- Grossberg, S., Pribe, C. & Cohen, M. A. (1997). Neural control of interlimb oscillations. I: Human bimanual coordination. *Biological Cybernetics*, 77, 131–140.
- Haken, H., Kelso, J. A. S. & Bunz, H. (1985). A theoretical model of phase transitions in human hand movements. *Biological Cybernetics*, 51, 347–356.
- Hallett, M., Shahani, B. T. & Young, R. R. (1977). Analysis of stereotyped voluntary movements at the elbow in Parkinson's disease. *Journal of Neurology, Neurosurgery, and Psychiatry*, 40, 1129–1135.
- Hoff, B. & Arbib, M. A. (1993). Models of trajectory formation and temporal interaction of reach and grasp. *Journal of Motor Behavior*, 25 (3), 175–192.
- Hogan, N. (1984). An organizing principle for a class of voluntary movements. *Journal of Neuroscience*, 4 (11), 2745–2754.
- Hollerbach, J. M. (1981). An oscillation theory of handwriting. *Biological Cybernetics*, 39, 139–156.
- Iberall, A. (1972). *Toward a general science of viable systems*. New York: McGraw-Hill.
- Jeannerod, M. (1984). The timing of natural prehension movements. *Journal of Motor Behavior*, 16, 723–745.
- Kalveram, K.-T. (1998). A neural oscillator model learning given trajectories, or how an alloimitation algorithm can be implemented into a motor controller. In J. Piek (Ed.), *Motor behavior and human skill*. Champaign, IL: Human Kinetics.
- Kay, B. A., Kelso, J. A. S., Saltzman, E. L. & Schöner, G. (1987). Space-time behavior of single and bimanual rhythmic movements: Data and limit cycle model. *Journal of Experimental Psychology: Human Perception and Performance*, 13, 178–192.
- Kelso, J. A. S. (1995). *Dynamic patterns: The self-organization of brain and behavior*. Cambridge, MA: MIT Press.

- Kelso, J. A. S., Fuchs, A. & Jirsa, V. K. (1999). Traversing scales of brain and behavioral organization. I: Concepts and experiments. In C. Uhl (Ed.), *Analysis of neurophysiological brain functioning*. Berlin: Springer.
- Kopell, N. (1993). Toward a theory of modelling pattern generators. In A. H. Cohen, S. Rossignol & S. Grillner (Eds.), *Neural control of rhythmic movements in vertebrates* (pp. 369–413). New York: Wiley.
- Lacquaniti, F., Terzuolo, C. & Viviani, P. (1983). The law relating the kinematic and figural aspects of drawing movements. *Acta Psychologica*, *54*, 115–130.
- Latash, M.L. (1993). *Control of human movement*. Champaign, IL: Human Kinetics.
- Latash, M. L. (2000). Modulation of simple reaction time on the background of an oscillatory action: Implications for synergy organization. *Experimental Brain Research*, *131*, 85–100.
- Matsuoka, K. (1985). Sustained oscillations generated by mutually inhibiting neurons with adaptations. *Biological Cybernetics*, *52*, 367–376.
- Matsuoka, K. (1987). Mechanisms of frequency and pattern control in the neural rhythm generators. *Biological Cybernetics*, *56*, 345–353.
- Rall, W. (1995). Perspective on neuron model complexity. In M. Arbib (Ed.), *Handbook of brain theory and neural networks* (pp. 728–732). Cambridge, MA: MIT Press.
- Saltzman, E. & Kelso, J. A. S. (1987). Skilled actions: a task-dynamic approach. *Psychological Review*, *94* (1), 84–106.
- Schaal, S. & Sternad, D. (1998). *Programmable pattern generators*. Paper presented at the International Conference on Computational Intelligence in Neuroscience (ICCIN '98), ResearchTriangle Park, NC, 24–26 October.
- Schaal, S. & Sternad, D. (2001). Origins and violations of the 2/3 power law in rhythmic 3D arm movements. *Experimental Brain Research*, *136* (1), 60–72.
- Schöner, G. (1990). A dynamic theory of coordination of discrete movement. *Biological Cybernetics*, *63*, 257–270.
- Schöner, G. (1995). From interlimb coordination to trajectory formation: Common dynamical principles. In S. Swinnen, H. Heuer, J. Massion & P. Casaer (Eds.), *Interlimb coordination: Neural, dynamical and cognitive constraints* (pp. 339–368). San Diego, CA: Academic Press.
- Softky, W. & Koch, C. (1995). Single cell models. In M. Arbib (Ed.), *The handbook of brain theory and neural networks* (pp. 879–884). Cambridge, MA: MIT Press.
- Soodak, H. & Iberall, A. S. (1972). Homeokinetics: a physical science for complex systems. *Science*, *201*, 579–582.
- Staupe, G., Wolf, W., Ott, M., Oertel, W. H. & Dengler, R. (1995). Tremor as a factor in prolonged reaction times of Parkinsonian patients. *Movement Disorders*, *10* (2), 153–162.
- Sternad, D., Amazeen, E. L. & Turvey, M. T. (1996). Diffusive, synaptic, and synergetic coupling: An evaluation through inphase and antiphase rhythmic movements. *Journal of Motor Behavior*, *28*, 255–269.
- Sternad, D., Saltzman, E. L. & Turvey, M. T. (1998). Interlimb coordination in a simple serial behavior: A task dynamic approach. *Human Movement Science*, *17*, 393–433.
- Sternad, D. & Schaal, S. (1999). Segmentation of endpoint trajectories does not imply segmented control. *Experimental Brain Research*, *124* (1), 118–136.
- Turvey, M. T. (1990). Coordination. *American Psychologist*, *45*, 938–953.
- Uno, Y., Kawato, M. & Suzuki, R. (1989). Formation and control of optimal trajectory in human multijoint arm movement: Minimum torque-change model. *Biological Cybernetics*, *61*, 89–101.
- Viviani, P. & Terzuolo, C. (1982). Trajectory determines movement dynamics. *Neuroscience*, *7* (2), 431–437.
- Wierzbicka, M. M., Staupe, G., Wolf, W. & Dengler, R. (1993). Relationship between tremor and the onset of rapid voluntary contraction in Parkinson disease. *Journal of Neurology, Neurosurgery, and Psychiatry*, *56*, 782–787.

Winfree, A. T. (1990). *The geometry of biological time*. New York: Springer.

Yates, F. E., Marsh, D. J. & Iberall, A. S. (1972). Integration of the whole organism – a foundation for a theoretical biology. In J. A. Behnke (Ed.), *Challenging biological problems: Directions towards their solution* (pp. 110–132), New York: Oxford University Press.